NUMERICAL CHARACTERIZATION OF A NEW ENERGY TRANSPORT MODEL

Edwin C. Kan†*, Datong Chen‡, Umberto Ravaioli† and Robert W. Dutton‡
†*Beckman Institute, University of Illinois at Urbana-Champaign*
‡*Center for Integrated Systems, Stanford University*

ABSTRACT

The numerical aspects of an new Energy Transport (ET) model [1], which demonstrates competitive physical and numerical properties for submicron device simulation, are discussed. We first modify the discretization scheme for the improved formulation of diffusion terms in the ET model, which resolves the black-current problem in Stratton's model [1, 2] and the spurious velocity overshoot problem in hydrodynamic models [3]. The elimination of multiple solutions of carrier temperature resulting from a simplified mobility model [4] is then discussed. Finally we show the comparison in CPU time of typical diode and MOSFET simulations using the standard drift-diffusion (DD) model and the ET model.

I. INTRODUCTION

We have developed and implemented a new Energy Transport (ET) model [1], which has solved both the problem of non-zero black current in Stratton's model [2] and the problem of the artificial velocity overshoot in conventional hydrodynamic (HD) model [3]. The new ET model is based on an extended Stratton's approach [2] with approximations on the microscopic relaxation time τ and the even part of the distribution function f_0. In [1], we originally use a position-independent microscopic relaxation time $\tau = \tau(E) \propto E^{-p}$, where E is the carrier energy, and obtain the current expression for electrons as

$$\mathbf{J} = -q\mu n\nabla\psi + k_B\nabla(n\mu T_n) \tag{1}$$

where ψ is electrical potential, k_B the Boltzmann constant, n the electron concentration, μ the electron mobility and T_n the electron temperature. Notice that in (1) there exists a non-zero black current, which is defined as the current with no driving force (i.e., when $\nabla\psi = 0$, $\nabla n = 0$ and $\nabla T_n = 0$), due to the component $k_B n T_n \nabla\mu$ for common mobility models $\mu = \mu(\mathbf{r}, T_n)$. The HD model, due to its approach from macroscopic relaxation time approximation, usually does not include this component, but demonstrates a spurious velocity overshoot peak in typical $n^+ - n - n^+$ diode simulations [6]. The black current problem in (1) can be however resolved in consideration of the spatial dependence of the microscopic relaxation time τ. In device applications with inhomogeneous impurity and surface phonon scatterings, we can generalize the assumption on τ by $\tau = \tau(\mathbf{r}, E)$, where $\mathbf{r}$ represents the spatial coordinates. With the approximations used in [1], which includes the non-Maxwellian distribution and nonparabolic bands, the current can now be written as

$$\mathbf{J} = -q\mu n\nabla\psi + k_B\mu\nabla(nT_n) + k_B n T_n \frac{\partial\mu(\mathbf{r}, T_n)}{\partial T_n}\nabla T_n \tag{2}$$

In comparison with (1), it indicates that in the formulation of the diffusion term, the explicit spatial derivative of μ is not a proper driving force of the current, while the electron-temperature

*E. C. Kan is now with Dawn Technologies, Inc., 491 Macara Ave., Suite 1002, Sunnyvale, CA 94086

derivative of μ is, so that the nonzero black current present in (1) is eliminated in (2).

II. DISCRETIZATION

The electron mobility is usually expressed in an empirical formulation (see, for example, [4, 5])

$$\mu(\mathbf{r}, T_n) = \mu(\mu_0(\mathbf{r}), T_n) \,. \tag{3}$$

where $\mu_0(\mathbf{r})$ is the low field mobility. For this mobility model, the modification on discretization from (1) to (2) can be easily reflected in the self-consistent discretization scheme [1]. In [1], the normalized current along the mesh line l is originally written as

$$\tilde{J}_l = \frac{1}{L_{ij}} \left(B(\tilde{u}_{ij}) \tilde{n}_j \mu(x_j, \tilde{T}_j) \tilde{T}_j - B(-\tilde{u}_{ij}) \tilde{n}_i \mu(x_i, \tilde{T}_i) \tilde{T}_i \right) \tag{4}$$

where the tilde mark denotes the normalized quantities, L_{ij} is the distance between nodes i and j, $B(u) = u/(exp(u) - 1)$ is the Bernoulli function, $\tilde{u}_{ij} = 2(\psi_j - \psi_i)/(\tilde{T}_i + \tilde{T}_j)$, and $\mu(x, \tilde{T}) = \mu(\mu_0(x), \tilde{T})$. All of the above notations of variables follow those in [1].

Notice that, in mobility model (3), all explicit spatial dependence of μ is included in $\mu_0(x)$. Therefore in addition to the assumptions of constant $\bar{J}$, $\bar{S}$ and $(1/T)(d\psi/dl)$ in [1], we can further assume μ_0 is constant along the mesh line, $\bar{\mu}_0 = (\mu_0(x_i) + \mu_0(x_j))/2$ (also used in conventional Scharfetter-Gummel scheme for the drift-diffusion model), to reflect the elimination of the explicit spatial derivative of μ in new formulation (2). Using these assumptions, we can discretize (2) along l and obtain

$$\tilde{J}_l = \frac{1}{L_{ij}} \left(B(\tilde{u}_{ij}) \tilde{n}_j \mu(\bar{\mu}_0, \tilde{T}_j) \tilde{T}_j - B(-\tilde{u}_{ij}) \tilde{n}_i \mu(\bar{\mu}_0, \tilde{T}_i) \tilde{T}_i \right) \,. \tag{5}$$

The corresponding diffusion part in the energy flux S can be treated similarly, and the normalized energy flux along l can be written as

$$\tilde{S}_l = \frac{1}{L_{ij}} \left(B(\tilde{u}_{ij}) \tilde{n}_j \mu(\bar{\mu}_0, \tilde{T}_j) \tilde{T}_j^2 - B(-\tilde{u}_{ij}) \tilde{n}_i \mu(\bar{\mu}_0, \tilde{T}_i) \tilde{T}_i^2 \right) \,. \tag{6}$$

The elegant parallel between the discretized J and S [1] is preserved.

Since PISCES II evaluates its low-field mobility μ_0 at the intermesh points, the numerical results presented in [1] actually use (2) instead of (1), where the spurious velocity overshoot of the HD model in the simulation of typical $n^+ - n - n^+$ diodes nearly vanished.

III. IMPLEMENTATION

Since the ET model bears very similar numerical structure to the conventional DD model, the migration from the DD based simulation program such as PISCES is not difficult. However, the uniqueness of the solution in the ET model has been perturbed from the DD model owing to the additional energy balance equation. This can be understood from the following simplified analysis. Because of the velocity saturation effects, $\mu(\mathbf{r}, T_n)$ will asymptotically tend to T_n^{-1} in high fields. The energy balance equation, which can be written as

$$\nabla \cdot \mathbf{S} = \mathbf{F} \cdot \mathbf{J} - \frac{3 k_B n}{2} \frac{T_n - T_0}{\tau_\epsilon} \,, \tag{7}$$

is quadratic in T_n if the energy relaxation time τ_ϵ is nearly independent of T_n, which is appropriate for Si as shown by Monte Carlo calculations. This quadratic nature may give two possible values of T_n (one is nonphysical and temporally unstable) symmetric about T_0. This will imply nonuniqueness of the solution of the partial differential equation system. For some types of iteration schemes it is indeed possible to obtain occasionally such nonphysical solution, one example of which is given in Fig. 1, where T_n at the 0.3μm cross section away from the channel of a submicron MOSFET is plotted. We can observe in some region T_n is indeed smaller than T_0. To correct this problem and ensure physical solutions, we can add penalty functions for nonphysical temperatures, such as $ae^{b(T_0-T_n)}$ with a and b being some appropriate positive constants chosen not to affect the precision of the original absolute residual. This scheme is applied to the same situation where the nonphysical T_n is observed using the same initial guess and convergence method. The result is also shown in Fig. 1.

IV. NUMERICAL CHARACTERISTICS

We have tested the ET model in a version of the simulator, PISCES, using the full Newton method. The convergence property is shown in Fig. 2 for typical cases of one-carrier and two-carrier solutions. The second-order convergence rate of the discretization scheme is observed. The CPU time and resident memory requirement in comparison with the standard drift-diffusion (DD) model running on the same structures and meshes are summarized in Fig. 3. All simulations are performed on a SUN Sparc Work Station. The ET model is approximately 3-4 times slower than the DD model and requires 1.5 times larger resident memory. In consideration of today's hardware capabilities, the ET model is very promising to simulate the nonlocal transport effects in future device applications.

References

[1] D. Chen, E. C. Kan, U. Ravaioli, C.-W. Shu and R. W. Dutton, *IEEE Electron Device Lett.*, vol. 13, no. 1, pp. 26-28, 1992.

[2] R. Stratton, *Phys. Rev.*, vol. 126, no. 6, pp. 2002-2014, 1962.

[3] E. Fatemi, J. Jerome and S. Osher, *IEEE Trans. Computer-Aided Design,* vol. 10, no. 2, pp. 232-244, 1991.

[4] G. Baccarani and M. R. Wordeman, *Solid State Electron.*, vol. 28, no. 4, pp. 407-416, 1985.

[5] S. Selberherr, *Analysis and Simulation of Semiconductor Devices,* Vienna: Springer, 1984.

[6] D. Chen, E. Sangiorgi, M. Pinto, E. C. Kan, U. Ravaioli and R. W. Dutton, *to be presented at NUPAD 92.*

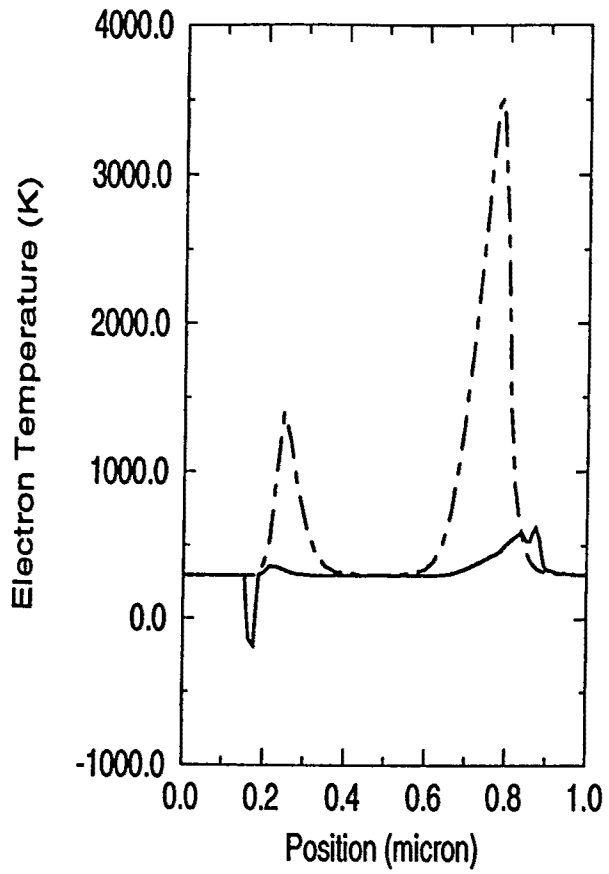

Fig. 1. Demonstration of multiple solutions of T_c. Solid: T_c without using the penalty functions; dash-dot: T_c with penalty functions. The results are obtained from a cross-section near the depletion edge of a $0.4\mu m$-channel MOSFET structure.

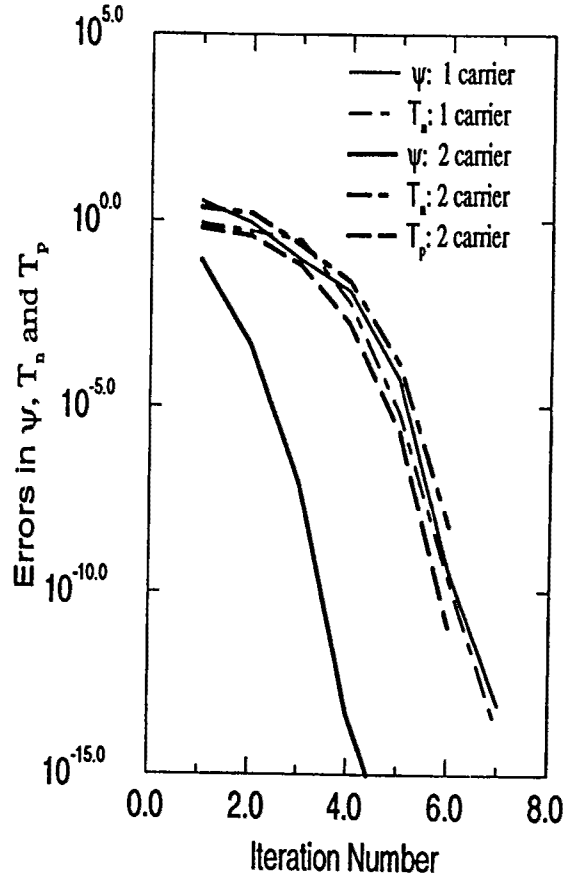

Fig. 2. Convergence property of a typical numerical experiment of the new ET model. Both one-carrier simulation on $n^+ - n - n^+$ structures and two-carrier simulation on BJT structures are shown. The potential ψ and the carrier temperatures T_n and T_p are in arbitary units. The error is calculated by the second norm of the correction vector.

device	one-carrier $n^+ - n - n^+$		two-carrier BJT	
mesh points	100×2		30×25	
model	DD	ET	DD	ET
one bias point (s)	0.76	3.01	16.73	90.61
three bias points (s)	3.86	12.05	55.08	213.69
max. resident memory (kb)	836	1,448	3,356	5,072

Fig. 3. Comparison of CPU time and maximum resident memory requirement using the standard DD and the new ET models. The results are obtained from PISCES using the full newton method.